

1 **Structural signatures of igneous sheet intrusion propagation**

2
3 Craig Magee^{a*}, James Muirhead^b, Nick Schofield^c, Richard Walker^d, Olivier Galland^e, Simon
4 Holford^f, Juan Spacapan^g, Christopher A-L Jackson^a, William McCarthy^h

5
6 ^aBasins Research Group, Department of Earth Science and Engineering, Imperial College
7 London, London, SW7 2BP, UK

8 ^bDepartment of Geological Sciences, University of Idaho, Moscow, Idaho, 83844, USA

9 ^cGeology & Petroleum Geology, School of Geosciences, University of Aberdeen, Aberdeen,
10 AB24 3UE, UK

11 ^dSchool of Geography, Geology, and the Environment, University of Leicester, Leicester,
12 LE1 7RH, UK

13 ^ePhysics of Geological Processes (PGP), Department of Geosciences, University of Oslo,
14 Blindern, 0316 Oslo, Postbox 1048, Norway

15 ^fAustralian School of Petroleum, University of Adelaide, Adelaide, SA 5005, Australia

16 ^gUniversidad Nacional de La Plata-CONICET-Fundación YPF, 1900 La Plata, Argentina

17 ^hDepartment of Earth Sciences, University of St Andrews, St Andrews, KY16 9AL, UK

18
19 *corresponding author: c.magee@imperial.ac.uk (+44 (0)20 7594 6510)

21 **Abstract**

22 The geometry and distribution of igneous dykes, sills, and inclined sheets has long been used
23 to determine emplacement mechanics, define melt source locations, and reconstruct
24 palaeostress conditions to shed light on various tectonic and magmatic processes. Since the
25 1970's we have recognised that sheet intrusions do not necessarily display a continuous,
26 planar geometry, but commonly consist of segments. The morphology of these segments and

27 their connectors, is controlled by, and provide insights into the behaviour, of the host rock
28 during emplacement: (i) brittle fracturing leads to the formation of intrusive steps or bridge
29 structures between adjacent segments; and (ii) brittle shear and flow processes, as well as
30 non-brittle heat-induced viscous flow or fluidization, promotes magma finger development.
31 Textural indicators of magma flow (e.g., rock fabrics) reveal that segments are aligned
32 parallel to the initial sheet propagation axis. Recognising and mapping segment long axes
33 thus allows melt source location hypotheses, derived from sheet distribution and orientation,
34 to be robustly tested. Despite the information that can be obtained from these structural
35 signatures of sheet intrusion propagation, they are largely overlooked by the structural and
36 volcanological communities. To highlight their utility, we briefly review the formation of
37 sheet intrusion segments, discuss how they inform interpretations of magma emplacement,
38 and outline future research directions.

39

40 **1. Introduction**

41 Igneous sheet intrusions are broadly planar bodies (e.g., dykes, sills, and inclined sheets) that
42 facilitate magma flow through Earth's crust. Because their distribution and geometry is
43 considered to be controlled by the principal stress axes during emplacement, with intrusion
44 walls typically orienting orthogonal to σ_3 within the σ_1 - σ_2 plane, mapping igneous sheet
45 swarms is used to identify magma source locations, reconstruct palaeogeographies, and
46 determine syn-emplacement stress conditions (e.g., Anderson, 1936; Anderson, 1951; Ernst
47 et al., 1995; Rubin, 1995; Muirhead et al., 2015). The link between intrusion geometry and
48 contemporaneous stress field conditions has thus underpinned and dominated research and
49 teaching of igneous sheet emplacement in the fields of structural geology and volcanology.

50 Over the last 50 years, it has been recognised that most igneous sheet intrusions
51 consist of segments (e.g., Pollard et al., 1975; Delaney and Pollard, 1981; Rickwood, 1990;

52 Schofield et al., 2012a), similar to structures observed in clastic intrusions (e.g., Vétel and
53 Cartwright, 2010) and mineralized veins (e.g., Nicholson and Pollard, 1985). The majority of
54 research has focused on segmented dykes emplaced via tensile elastic fracturing of the host
55 rock (e.g., Delaney and Pollard, 1981; Rickwood, 1990), but several studies have
56 demonstrated that brittle shear and flow, as well as viscous host rock deformation, during sill
57 intrusion can also promote segmentation (e.g., Pollard et al., 1975; Hutton, 2009; Schofield et
58 al., 2010; Spacapan et al., 2017). Segmentation of igneous sheets is documented across at
59 least five orders of magnitude in scale, from intrusions that are a few centimetres to hundreds
60 of meters thick, suggesting that segment formation and linkage are scale independent
61 (Schofield et al., 2012a). Variable segment morphologies (e.g., magma fingers; Pollard et al.,
62 1975; Schofield et al., 2010), as well as that of the potential connectors between segments
63 (e.g., intrusive steps, broken bridges; Rickwood, 1990), produce the broader sheet geometry
64 and reflect the mechanical processes that facilitate emplacement (Schofield et al., 2012a).
65 Rock fabric analyses of primary magma flow structures (e.g., chilled margin magnetic
66 fabrics) have shown that the long axes of segments and their connectors typically parallel the
67 principal axis of initial sheet propagation (e.g., Baer and Reches, 1987; Rickwood, 1990;
68 Baer, 1995; Liss et al., 2002; Magee et al., 2012; Hoyer and Watkeys, 2017). Identification
69 and analysis of segments and connectors in the field and in seismic reflection data thus
70 provides a simple way to map primary magma propagation patterns and determine syn-
71 emplacement host rock behaviour (e.g., Rickwood, 1990; Schofield et al., 2012a; Schofield et
72 al., 2012b). Here, our aim is to: (i) summarise our current understanding of magma segment
73 formation; (ii) highlight how these structures can be used to unravel controls on magma flow
74 through Earth's crust; and (iii) outline future research directions.

75 **2. Primary magma flow indicators**

76 *2.1. Intrusive steps and bridge structures formed by tensile brittle fracturing*

77 Regardless of their orientation or propagation direction, many sheet intrusions exhibit a
78 stepped geometry consisting of sub-parallel segments that are slightly offset from one another
79 and may overlap (Figs 1-3) (e.g., Delaney and Pollard, 1981; Rickwood, 1990; Schofield et
80 al., 2012a). It is broadly accepted that stepped intrusion geometries result from segmentation
81 of a propagating tensile elastic fracture, i.e. oriented orthogonal to σ_3 , immediately ahead of
82 an advancing sheet intrusion (e.g., Delaney and Pollard, 1981; Baer, 1995). As magma fills
83 the fracture, segments begin to inflate and widen through lateral tip propagation, promoting
84 tensile fracture of the intervening host rock and eventual segment coalescence (Fig. 1A) (e.g.,
85 Rickwood, 1990; Hutton, 2009; Schofield et al., 2012a). Structural signatures of this
86 segmentation are controlled by segment offset, which describes the strike-perpendicular
87 distance between the planes of two segments, and overlap, which can be negative (i.e.
88 underlap) and describes the strike-parallel distance between segment tips (Fig. 1A) (cf.
89 Delaney and Pollard, 1981; Rickwood, 1990). We also introduce ‘stepping direction’, which
90 can either be consistent or inconsistent, to define the relative offset direction of adjacent
91 segments (Fig. 1B).

92 When viewed in a 2D cross-section (e.g., an outcrop), segments typically appear
93 unconnected at their distal end, away from the magma source, whereas increased magma
94 supply in proximal locations promotes their inflation and coalescence to form a continuous
95 sheet intrusion (Fig. 1A) (Rickwood, 1990; Schofield et al., 2012a; Schofield et al., 2012b).
96 Connectors between segments are classified as intrusive steps, if the segment overlap is
97 neutral or negative, or bridge structures when segments overlap (Figs 1-3). Changes in
98 overlap along segment long axes may mean steps transition into bridge structures and vice
99 versa (Schofield et al., 2012a; Schofield et al., 2012b). Variations in the degree and style of
100 segment connectivity with distance from the magma source imply that the segmentation
101 process results from initial sheet propagation dynamics (Schofield et al., 2012a).

102

103 *2.1.1. Fracture segmentation*

104 Two processes are commonly invoked to explain the development of initially unconnected
105 fracture segments: (i) syn-emplacement rotation of the principal stress axes orientations (e.g.,
106 Pollard et al., 1982; Nicholson and Pollard, 1985; Takada, 1990); and (ii) exploitation of
107 preferentially oriented, pre-existing structures (Hutton, 2009; Schofield et al., 2012a).
108 Geological systems likely display a combination of these segmentation mechanisms, and
109 potentially others, so it is therefore important to understand the characteristics of each process
110 to decipher their relative contributions.

111 In the first scenario, a change in the principal stress axes orientation ahead of a
112 propagating fracture, likely due to the onset of mixed mode loading (mode I+II or mode
113 I+III), causes it to twist and split into en echelon segments that strike orthogonal to the
114 locally reoriented σ_3 axis (Fig. 4A) (Pollard et al., 1982; Nicholson and Pollard, 1985; Cooke
115 et al., 1999). This segmentation of mixed mode fractures is dictated by the maximum
116 circumferential stress direction, direction of maximum energy release, maximum principal
117 stress, direction of strain energy minimum, and the symmetry criterion (Cooke et al., 1999).
118 The plane broadly defined by the overall geometry of the en echelon segments remains
119 parallel to the orientation of the original fracture (Fig 4A) (Rickwood, 1990). Steps and
120 bridge structures generated due to this style of segmentation have a consistent stepping
121 direction (e.g., Fig. 1B).

122 The second mechanism for step and bridge formation involves exploitation of
123 preferentially oriented (i.e. with respect to the contemporaneous principal stress axes), pre-
124 existing structures by propagating fractures/intrusions (e.g., Hutton, 2009; Schofield et al.,
125 2012a). For example, many sills emplaced into sedimentary strata can be divided into
126 segments that exploited different bedding planes in an attempt to find the least resistant

127 pathway (e.g., Figs 2D and 3A) (Hutton, 2009). Bedding planes are particularly exploited
128 because they: (i) exhibit relatively lower tensile strength and fracture toughness compared to
129 intact rock (e.g., Schofield et al., 2012a; Kavanagh and Pavier, 2014); and/or (ii) mark a
130 significant mechanical contrast in intact rock properties (e.g., Poisson's ratio, Young's
131 modulus) that localises strain (e.g., Kavanagh et al., 2006; Gudmundsson, 2011). In contrast
132 to en echelon segments, the stepping direction of intrusions exploiting different pre-existing
133 weaknesses may be inconsistent (Figs 1B and 3E) (Schofield et al., 2012a).

134 Alternative mechanisms that may account for segmentation and step formation
135 involve: (i) development of high stress intensities at the leading edge of an intruding sheet,
136 promoting rapid crack propagation and formation of a fracture morphology, with a consistent
137 stepping direction, akin to hackle marks (Fig. 4B) (Schofield et al., 2012a); or (ii) the
138 occurrence of low or zero-cohesion, pre-existing structures (e.g., faults), striking orthogonal
139 to the sheet propagation direction, which can promote segmentation and provide a pathway
140 for magma to form a fault-parallel step (Magee et al., 2013; Stephens et al., 2017). The
141 stepping direction of sills influenced by pre-existing faults is controlled by the fault dip
142 direction relative to the sheet propagation direction (Magee et al., 2013). In these scenarios,
143 the stepped fracture plane is continuous and thus allows the magma to propagate as a single
144 sheet; bridge structures cannot form via these processes because segments do not overlap
145 (e.g., Fig. 4B).

146

147 *2.1.2. Host rock deformation and bridge development*

148 When segments overlap, their inflation may be accommodated by bending of the intervening
149 host rock bridge (Figs 1A and 3) (Farmin, 1941; Nicholson and Pollard, 1985; Rickwood,
150 1990; Hutton, 2009). The monoformal folding of the host rock bridge records a tangential
151 longitudinal strain relative to the orientation of the folded layers and induces outer-arc

152 extension and inner-arc compression along the fold convex and concave surfaces,
153 respectively (Hutton, 2009; Schofield et al., 2012a). As magma inflation continues, outer-arc
154 extension increases and may exceed the tensile strength of the intact host rock, promoting
155 development of extension fractures across the bridge (Figs 3B and C) (e.g., Hutton, 2009;
156 Schofield et al., 2012b). Fractures cross-cutting unfolded bridge structures may also form if
157 local crack-induced stresses at segment tips are sufficiently high to promote fracture rotation
158 and propagation towards each other (e.g., Fig. 3D) (e.g., Olson and Pollard, 1989). Continued
159 fracture growth and infilling by magma can separate the bridge from one or both sides to
160 form a broken bridge (Fig. 3B) or a bridge xenolith (Fig. 3D), respectively (Hutton, 2009).

161

162 *2.2. Magma finger formation through brittle and/or non-brittle processes*

163 In contrast to established tensile brittle fracturing models, several studies have demonstrated
164 that magma may intrude via brittle (i.e. shear and flow) and non-brittle processes (e.g.,
165 Pollard et al., 1975; Duffield et al., 1986; Schofield et al., 2010; Schofield et al., 2012a;
166 Wilson et al., 2016). Such host rock deformation modes lead to the emplacement of magma
167 fingers; i.e. long, linear or sinuous, narrow segments that have blunt and/or bulbous
168 terminations (e.g., Pollard et al., 1975; Schofield et al., 2010; Schofield et al., 2012a;
169 Spacapan et al., 2017).

170 Sheet intrusion into unconsolidated or highly incompetent host rocks, where little
171 cohesion between grains and/or low shear moduli inhibits tensile brittle failure, can instigate
172 brittle flow of host rock grains and magma finger formation (e.g., Pollard et al., 1975;
173 Schofield et al. 2012a). Accommodation of magma by pore collapse particularly affects sheet
174 intrusions emplaced: (i) at shallow-levels in sedimentary basins where host rock sequences
175 have undergone little burial and/or diagenesis (e.g., Einsele et al., 1980; Morgan et al., 2008;

176 Schofield et al., 2012a); or (ii) in strata that have been prevented from undergoing normal
177 compaction with burial (Eide et al., 2017).

178 Shear failure of unconsolidated and relatively soft (e.g., shale) host rock by brittle
179 faulting and/or ductile deformation can also form and accommodate magma fingers (Fig. 5)
180 (e.g., Pollard, 1973; Duffield et al., 1986; Rubin, 1993; Spacapan et al., 2017). Kinematic
181 indicators of such compressional shear structures indicate that the intrusion ‘pushed’ into the
182 host rock, leading to confined rock wedging (Pollard, 1973; Rubin, 1993; Spacapan et al.,
183 2017). This hybrid shear brittle and non-brittle propagation mechanism, called viscous
184 indentation, is assumed to occur when the viscous shear stresses within a flowing magma,
185 near its intrusion tip, are transferred to and promote shear failure of the host rock (Fig. 5)
186 (Galland et al., 2014). Viscous indentation is therefore expected to primarily accommodate
187 emplacement of viscous, intermediate to felsic magma (Donnadiu and Merle, 1998; Merle
188 and Donnadiu, 2000).

189 Intrusion-induced heating (i.e. primary non-brittle emplacement) can cause some host
190 rocks, particularly evaporites and bituminous coals, to behave as a high viscosity fluid (i.e.
191 fluidisation), the plastic deformation of which allows low viscosity melt injections to form
192 magma fingers (e.g., Fig. 6) (Schofield et al., 2010; Schofield et al., 2012a; Schofield et al.,
193 2014). Magma fingers can also form by fluidization of coherent, mechanically competent
194 host rock (e.g., Pollard et al., 1975; Schofield et al. 2012a); i.e. secondary induced non-brittle
195 magma emplacement (Schofield et al., 2012a). Two secondary induced non-brittle
196 emplacement scenarios may be considered whereby magma intrusion can: (i) promote *in situ*
197 boiling and volatisation of pore-fluids via heating (i.e. thermal fluidization); or (ii) open
198 fractures that rapidly depressurize pore-fluids, which expand and catastrophically
199 disaggregate the host rock (Schofield et al., 2010; Schofield et al., 2012a).

200

201 **3. Discussion**

202 Having described how segmentation occurs and is structurally accommodated, here we
203 discuss selected examples of how this knowledge has been applied and highlight possible
204 future directions.

205

206 *3.1. Lateral magma flow in mafic sill-complexes*

207 The current paradigm describing crustal magma transport broadly involves the vertical ascent
208 and/or lateral intrusion of dykes (e.g., Gudmundsson, 2006; Cashman and Sparks, 2013).

209 However, recent field- and seismic-based studies that infer magma flow patterns from
210 segment long axes and/or rock fabric analyses within interconnected networks of mafic sills
211 and inclined sheets (i.e. sill-complexes), demonstrate that these systems can facilitate
212 significant vertical (up to 12 km) and lateral (up to 4000 km) magma transport (e.g.,
213 Cartwright and Hansen, 2006; Leat, 2008; Muirhead et al., 2014; Magee et al., 2016). The
214 lateral growth of such sill-complexes has been shown to control vent migrations and,
215 potentially, transitions from effusive to explosive volcanism in active and extinct mafic
216 monogenetic volcanic fields (e.g., Kavanagh et al., 2015; Muirhead et al., 2016). Mapping
217 segment long axes suggests that sill-complexes may be as important as dykes in various
218 tectonic, magmatic, and volcanic processes (Magee et al., 2016).

219

220 *3.2. Intrusion opening vectors*

221 Over a century of research has led to the prescribed dogma that sheet opening exclusively
222 involves tensile dilation of Mode I fractures (e.g., Anderson, 1936): Intrusion planes are
223 therefore expected to orient orthogonal to σ_3 , which is a function of the interplay between far-
224 field and local stress fields (e.g., Anderson, 1936; Anderson, 1951; Odé, 1957; Gautneb and
225 Gudmundsson, 1992; Geshi, 2005). However, from analysing sheet segmentation processes,

226 it is clear that several brittle (e.g., shear and flow) and non-brittle (e.g., fluidisation) processes
227 can accommodate the emplacement of intrusions that may not strike orthogonal to σ_3 (e.g.,
228 Schofield et al., 2012a; Schofield et al., 2014). Although often overlooked, it is therefore
229 important to test the validity of the assumed relationship between sheet and σ_3 orientation,
230 through analysis of intrusion opening vectors (e.g., Walker, 1993; Jolly and Sanderson, 1997;
231 Walker, 2016; Walker et al., 2017). Importantly, the geometry of segment connectors
232 provides a record of local intrusion opening vectors (e.g., Olson and Pollard, 1989; Walker,
233 1993; Jolly and Sanderson, 1995; Cooke and Pollard, 1996; Stephens et al., 2017). Steps
234 formed during pure tensile opening of parallel magma segments should have virtually zero
235 thickness and simply accommodate shear displacement on a plane orthogonal to the sheet
236 intrusion plane (e.g., Figs 2A and C) (e.g., Stephens et al., 2017). Conversely, thick steps
237 require an opening vector that was *not* orthogonal to the intrusion plane (e.g., Fig. 2D)
238 (Walker et al., 2017). Whilst opening vectors of individual connectors may largely reflect
239 local stress fields related to crack-tip processes (e.g., Olson and Pollard, 1989), identifying
240 and collating such opening vector measurements across a sheet intrusion swarm can provide a
241 more robust test of the syn-emplacement stress conditions than analyses of sheet orientation
242 alone (Jolly and Sanderson, 1997; Walker et al., 2017).

243

244 *3.3. Bridge structures and relay zones*

245 As with intrusions, faults and fractures grow through stages of nucleation and linkage of
246 multiple discontinuous segments (e.g., Cartwright et al., 1996; Walsh et al., 2003). The
247 amount of overlap and offset of fault or fracture segments, and the existence of pre-existing
248 structure, leads to different styles of deformation in the intervening *relay zone* that
249 accommodates displacement gradients between fault segments (e.g., Tentler and Acocella,
250 2010). Despite the apparent similarity of relay zones and bridge structures (Schofield et al.,

251 2012b), few comparisons exist between the resulting ancillary structures associated with
252 segmented faults and segmented intrusions. Whilst relay zones have received considerable
253 attention in the literature (e.g., Peacock and Sanderson, 1991; Long and Imber, 2011), to our
254 knowledge there is no catalogue of overlap, offset, and strain parameters for bridge
255 structures. We suggest that systematic study of bridge structures, and comparison to relay
256 zones, could yield important constraints on shared processes.

257

258 **4. Conclusion**

259 Igneous sheet intrusions are not necessarily emplaced as continuous, planar bodies but
260 commonly develop through the coalescence of discrete magma segments. Segmentation can
261 be primarily attributed to either: (i) splitting of a tensile brittle fracture propagating ahead of a
262 sheet intrusion due to stress field rotations or exploitation of pre-existing weaknesses; (ii)
263 brittle shear and flow (i.e. pore collapse) deformation of poorly consolidated host rocks;
264 and/or (iii) non-brittle host rock fluidization. By briefly reviewing advances in our
265 understanding of sheet intrusion growth, we demonstrate how different emplacement
266 processes produce a variety of segment morphologies (e.g., magma fingers) and connecting
267 structures (e.g., steps and bridge structures), the long axes of which record the initial
268 fracture/magma propagation dynamics. We highlight how detailed mapping of sheet
269 segments can provide important clues regarding the distribution of melt sources, how magma
270 transits Earth's crust, mechanics of intrusion-induced host rock deformations, and
271 palaeostress states in various volcanic-tectonic environments.

272

273 **5. Acknowledgments**

274 CM acknowledges a Junior Research Fellowship funded by Imperial College London. JDM
275 acknowledges National Science Foundation grant EAR-1654518.

276

277 **6. Figure Captions**

278 Figure 1: (A) Schematic diagram documenting the description and development of segments
279 connected by steps and bridge structures (redrawn from Magee et al., 2016). (B) Schematic
280 diagram defining consistent and inconsistent stepping directions.

281

282 Figure 2: Steps developed in mafic sheets intruding: (A and B) Mesozoic limestone and shale
283 metasedimentary rocks on Ardnamurchan, NW Scotland; (C) Neoproterozoic schists at
284 Mallaig, NW Scotland; and (D) a sedimentary succession on Axel Heiburg island, Canada
285 (photo courtesy of Martin Jackson).

286

287 Figure 3: Different bridge structures recorded in mafic intrusions into: (A) Beacon
288 Supergroup sedimentary strata along the Theron Mountains, Antarctica (modified from
289 Hutton, 2009); (B) Beacon Supergroup sedimentary strata along the Allan Hills, Antarctica;
290 (C) a massive dolerite intrusion on Ardnamurchan, NW Scotland; and (D) Mesozoic
291 limestone and shale metasedimentary rocks on Ardnamurchan, NW Scotland. (E) Opacity
292 render of a sill in the Flett Basin, NE Atlantic and corresponding seismic sections detailed
293 intrusive step and broken bridge growth (modified from Schofield et al., 2012b).

294

295 Figure 4: (A) Schematic showing how a change in the principal stress axes can segment a
296 propagating sheet (after Hutton, 2009). (B) Hackle marks developed on a joint plane
297 (redrawn from Kulander et al., 1979).

298

299 Figure 5: Small-scale imbricate fold and thrust duplex developed due to viscous indentation
300 of finger-like sill intrusions in the Neuquén Basin, Argentina (modified from Spacapan et al.,
301 2017).

302

303 Figure 6: (A and B) Magma fingers developed in response to intrusion-induced heating and
304 plastic deformation of the host rock coals in the Raton Basin, Colorado (modified from
305 Schofield et al., 2012a). (C) Schematic diagrams showing the simplified 3D morphology of
306 the magma fingers in (A and B) (Schofield, 2009).

307

308 **7. References**

309 Anderson, E.M., 1936. Dynamics of formation of cone-sheets, ring-dykes, and cauldron
310 subsidence. *Proceedings of the Royal Society of Edinburgh* 56, 29.

311 Anderson, E.M., 1951. *The dynamics of faulting and dyke formation with applications to*
312 *Britain*. Hafner Pub. Co., Edinburgh.

313 Baer, G., 1995. Fracture propagation and magma flow in segmented dykes: field evidence
314 and fabric analyses, Makhtesh Ramon, Israel. *Physics and chemistry of dykes*. Balkema,
315 Rotterdam, 125-140.

316 Baer, G., Reches, Z.e., 1987. Flow patterns of magma in dikes, Makhtesh Ramon, Israel.
317 *Geology* 15, 569-572.

318 Cartwright, J.A., Hansen, D.M., 2006. Magma transport through the crust via interconnected
319 sill complexes. *Geology* 34, 929-932.

320 Cartwright, J.A., Mansfield, C., Trudgill, B., 1996. The growth of normal faults by segment
321 linkage. *Geological Society, London, Special Publications* 99, 163-177.

322 Cashman, K.V., Sparks, R.S.J., 2013. *How volcanoes work: A 25 year perspective*.

323 *Geological Society of America Bulletin* 125, 664-690.

324 Cooke, M.L., Mollema, P.N., Pollard, D.D., Aydin, A., 1999. Interlayer slip and joint
325 localization in the East Kaibab Monocline, Utah: field evidence and results from numerical
326 modelling. Geological Society, London, Special Publications 169, 23-49.

327 Cooke, M.L., Pollard, D.D., 1996. Fracture propagation paths under mixed mode loading
328 within rectangular blocks of polymethyl methacrylate. Journal of Geophysical Research:
329 Solid Earth 101, 3387-3400.

330 Delaney, P.T., Pollard, D.D., 1981. Deformation of host rocks and flow of magma during
331 growth of minette dikes and breccia-bearing intrusions near Ship Rock, New Mexico.
332 USGPO.

333 Donnadieu, F., Merle, O., 1998. Experiments on the indentation process during cryptodome
334 intrusions: new insights into Mount St. Helens deformation. Geology 26, 79-82.

335 Duffield, W.A., Bacon, C.R., Delaney, P.T., 1986. Deformation of poorly consolidated
336 sediment during shallow emplacement of a basalt sill, Coso Range, California. Bull Volcanol
337 48, 97-107.

338 Eide, C.H., Schofield, N., Jerram, D.A., Howell, J.A., 2017. Basin-scale architecture of
339 deeply emplaced sill complexes: Jameson Land, East Greenland. Journal of the Geological
340 Society 174, 23-40.

341 Einsele, G., Gieskes, J.M., Curray, J., Moore, D.M., Aguayo, E., Aubry, M.-P., Fornari, D.,
342 Guerrero, J., Kastner, M., Kelts, K., 1980. Intrusion of basaltic sills into highly porous
343 sediments, and resulting hydrothermal activity. Nature 283, 441-445.

344 Ernst, R., Head, J., Parfitt, E., Grosfils, E., Wilson, L., 1995. Giant radiating dyke swarms on
345 Earth and Venus. Earth-Science Reviews 39, 1-58.

346 Farmin, R., 1941. Host-rock inflation by veins and dikes at Grass Valley, California.
347 Economic Geology 36, 143-174.

348 Galland, O., Burchardt, S., Hallot, E., Mourgues, R., Bulois, C., 2014. Dynamics of dikes
349 versus cone sheets in volcanic systems. *Journal of Geophysical Research: Solid Earth* 119,
350 6178-6192.

351 Gautneb, H., Gudmundsson, A., 1992. Effect of local and regional stress fields on sheet
352 emplacement in West Iceland. *Journal of Volcanology and Geothermal Research* 51, 17.

353 Geshi, N., 2005. Structural development of dike swarms controlled by the change of magma
354 supply rate: the cone sheets and parallel dike swarms of the Miocene Otoge igneous complex,
355 Central Japan. *Journal of Volcanology and Geothermal Research* 141, 267-281.

356 Gudmundsson, A., 2006. How local stresses control magma-chamber ruptures, dyke
357 injections, and eruptions in composite volcanoes. *Earth-Science Reviews* 79, 1-31.

358 Gudmundsson, A., 2011. Deflection of dykes into sills at discontinuities and magma-chamber
359 formation. *Tectonophysics* 500, 50-64.

360 Hoyer, L., Watkeys, M.K., 2017. Using magma flow indicators to infer flow dynamics in
361 sills. *Journal of Structural Geology* 96, 161-175.

362 Hutton, D.H.W., 2009. Insights into magmatism in volcanic margins: bridge structures and a
363 new mechanism of basic sill emplacement - Theron Mountains, Antarctica. *Petroleum*
364 *Geoscience* 15, 269-278.

365 Jolly, R., Sanderson, D., 1997. A Mohr circle construction for the opening of a pre-existing
366 fracture. *Journal of Structural Geology* 19, 887-892.

367 Jolly, R., Sanderson, D.J., 1995. Variation in the form and distribution of dykes in the Mull
368 swarm, Scotland. *Journal of Structural Geology* 17, 1543-1557.

369 Kavanagh, J.L., Boutelier, D., Cruden, A., 2015. The mechanics of sill inception, propagation
370 and growth: Experimental evidence for rapid reduction in magmatic overpressure. *Earth and*
371 *Planetary Science Letters* 421, 117-128.

372 Kavanagh, J.L., Menand, T., Sparks, R.S.J., 2006. An experimental investigation of sill
373 formation and propagation in layered elastic media. *Earth and Planetary Science Letters* 245,
374 799-813.

375 Kavanagh, J.L., Pavier, M.J., 2014. Rock interface strength influences fluid-filled fracture
376 propagation pathways in the crust. *Journal of Structural Geology* 63, 68-75.

377 Kulander, B.R., Barton, C.C., Dean, S.L., 1979. Application of fractography to core and
378 outcrop fracture investigations. Department of Energy, Morgantown, WV (USA).
379 Morgantown Energy Research Center.

380 Leat, P.T., 2008. On the long-distance transport of Ferrar magmas. Geological Society,
381 London, Special Publications 302, 45-61.

382 Liss, D., Hutton, D.H., Owens, W.H., 2002. Ropy flow structures: A neglected indicator of
383 magma-flow direction in sills and dikes. *Geology* 30, 715-718.

384 Long, J.J., Imber, J., 2011. Geological controls on fault relay zone scaling. *Journal of*
385 *Structural Geology* 33, 1790-1800.

386 Magee, C., Jackson, C.A.-L., Schofield, N., 2013. The influence of normal fault geometry on
387 igneous sill emplacement and morphology. *Geology* 41, 407-410.

388 Magee, C., Muirhead, J.D., Karvelas, A., Holford, S.P., Jackson, C.A., Bastow, I.D.,
389 Schofield, N., Stevenson, C.T., McLean, C., McCarthy, W., 2016. Lateral magma flow in
390 mafic sill complexes. *Geosphere*, GES01256. 01251.

391 Magee, C., Stevenson, C., O'Driscoll, B., Schofield, N., McDermott, K., 2012. An alternative
392 emplacement model for the classic Ardnamurchan cone sheet swarm, NW Scotland,
393 involving lateral magma supply via regional dykes. *Journal of Structural Geology* 43, 73-91.

394 Merle, O., Donnadieu, F., 2000. Indentation of volcanic edifices by the ascending magma.
395 Geological Society, London, Special Publications 174, 43-53.

396 Morgan, S., Stanik, A., Horsman, E., Tikoff, B., de Saint Blanquat, M., Habert, G., 2008.
397 Emplacement of multiple magma sheets and wall rock deformation: Trachyte Mesa intrusion,
398 Henry Mountains, Utah. *Journal of Structural Geology* 30, 491-512.

399 Muirhead, J.D., Airolidi, G., White, J.D., Rowland, J.V., 2014. Cracking the lid: Sill-fed dikes
400 are the likely feeders of flood basalt eruptions. *Earth and Planetary Science Letters* 406, 187-
401 197.

402 Muirhead, J.D., Kattenhorn, S.A., Le Corvec, N., 2015. Varying styles of magmatic strain
403 accommodation across the East African Rift. *Geochemistry, Geophysics, Geosystems*.

404 Muirhead, J.D., Van Eaton, A.R., Re, G., White, J.D., Ort, M.H., 2016. Monogenetic
405 volcanoes fed by interconnected dikes and sills in the Hopi Buttes volcanic field, Navajo
406 Nation, USA. *Bull Volcanol* 78, 11.

407 Nicholson, R., Pollard, D., 1985. Dilation and linkage of echelon cracks. *Journal of Structural*
408 *Geology* 7, 583-590.

409 Odé, H., 1957. Mechanical Analysis of the Dike Pattern of the Spanish Peaks Area, Colorado.
410 *Geological Society of America Bulletin* 68, 567.

411 Olson, J., Pollard, D.D., 1989. Inferring paleostresses from natural fracture patterns: A new
412 method. *Geology* 17, 345-348.

413 Peacock, D., Sanderson, D., 1991. Displacements, segment linkage and relay ramps in normal
414 fault zones. *Journal of Structural Geology* 13, 721-733.

415 Pollard, D.D., 1973. Derivation and evaluation of a mechanical model for sheet intrusions.
416 *Tectonophysics* 19, 233-269.

417 Pollard, D.D., Muller, O.H., Dockstader, D.R., 1975. The form and growth of fingered sheet
418 intrusions. *Geological Society of America Bulletin* 86, 351-363.

419 Pollard, D.D., Segall, P., Delaney, P.T., 1982. Formation and interpretation of dilatant
420 echelon cracks. *Geological Society of America Bulletin* 93, 1291-1303.

421 Rickwood, P., 1990. The anatomy of a dyke and the determination of propagation and magma
422 flow directions. *Mafic dykes and emplacement mechanisms*, 81-100.

423 Rubin, A.M., 1993. Tensile fracture of rock at high confining pressure: implications for dike
424 propagation. *Journal of Geophysical Research: Solid Earth* 98, 15919-15935.

425 Rubin, A.M., 1995. Propagation of magma-filled cracks. *Annual Review of Earth and
426 Planetary Sciences* 23, 49.

427 Schofield, N., 2009. Linking sill morphology to emplacement mechanisms. University of
428 Birmingham.

429 Schofield, N., Alsop, I., Warren, J., Underhill, J.R., Lehné, R., Beer, W., Lukas, V., 2014.
430 Mobilizing salt: Magma-salt interactions. *Geology*, G35406. 35401.

431 Schofield, N., Heaton, L., Holford, S.P., Archer, S.G., Jackson, C.A.-L., Jolley, D.W., 2012b.
432 Seismic imaging of 'broken bridges': linking seismic to outcrop-scale investigations of
433 intrusive magma lobes. *Journal of the Geological Society* 169, 421-426.

434 Schofield, N., Stevenson, C., Reston, T., 2010. Magma fingers and host rock fluidization in
435 the emplacement of sills. *Geology* 38, 63-66.

436 Schofield, N.J., Brown, D.J., Magee, C., Stevenson, C.T., 2012a. Sill morphology and
437 comparison of brittle and non-brittle emplacement mechanisms. *Journal of the Geological
438 Society* 169, 127-141.

439 Spacapan, J.B., Galland, O., Leanza, H.A., Planke, S., 2017. Igneous sill and finger
440 emplacement mechanism in shale-dominated formations: a field study at Cuesta del
441 Chihuido, Neuquén Basin, Argentina. *Journal of the Geological Society* 174, 422-433.

442 Stephens, T., Walker, R., Healy, D., Bubeck, A., England, R., McCaffrey, K., 2017. Igneous
443 sills record far-field and near-field stress interactions during volcano construction: Isle of
444 Mull, Scotland. *Earth and Planetary Science Letters* 478, 159-174.

445 Takada, A., 1990. Experimental study on propagation of liquid-filled crack in gelatin: Shape
446 and velocity in hydrostatic stress condition. *Journal of Geophysical Research: Solid Earth* 95,
447 8471-8481.

448 Tentler, T., Acocella, V., 2010. How does the initial configuration of oceanic ridge segments
449 affect their interaction? Insights from analogue models. *Journal of Geophysical Research:*
450 *Solid Earth* 115.

451 Vétel, W., Cartwright, J., 2010. Emplacement mechanics of sandstone intrusions: insights
452 from the Panoche Giant Injection Complex, California. *Basin Research* 22, 783-807.

453 Walker, G.P.L., 1993. Re-evaluation of inclined intrusive sheets and dykes in the Cuillins
454 volcano, Isle of Skye. *Geological Society, London, Special Publications* 76, 489-497.

455 Walker, R., Healy, D., Kawanzaruwa, T., Wright, K., England, R., McCaffrey, K., Bubeck,
456 A., Stephens, T., Farrell, N., Blenkinsop, T., 2017. Igneous sills as a record of horizontal
457 shortening: The San Rafael subvolcanic field, Utah. *Geological Society of America Bulletin*,
458 B31671. 31671.

459 Walker, R.J., 2016. Controls on transgressive sill growth. *Geology* 44, 99-102.

460 Walsh, J., Bailey, W., Childs, C., Nicol, A., Bonson, C., 2003. Formation of segmented
461 normal faults: a 3-D perspective. *Journal of Structural Geology* 25, 1251-1262.

462 Wilson, P.I., McCaffrey, K.J., Wilson, R.W., Jarvis, I., Holdsworth, R.E., 2016. Deformation
463 structures associated with the Trachyte Mesa intrusion, Henry Mountains, Utah: Implications
464 for sill and laccolith emplacement mechanisms. *Journal of Structural Geology* 87, 30-46.

465

Figure 1

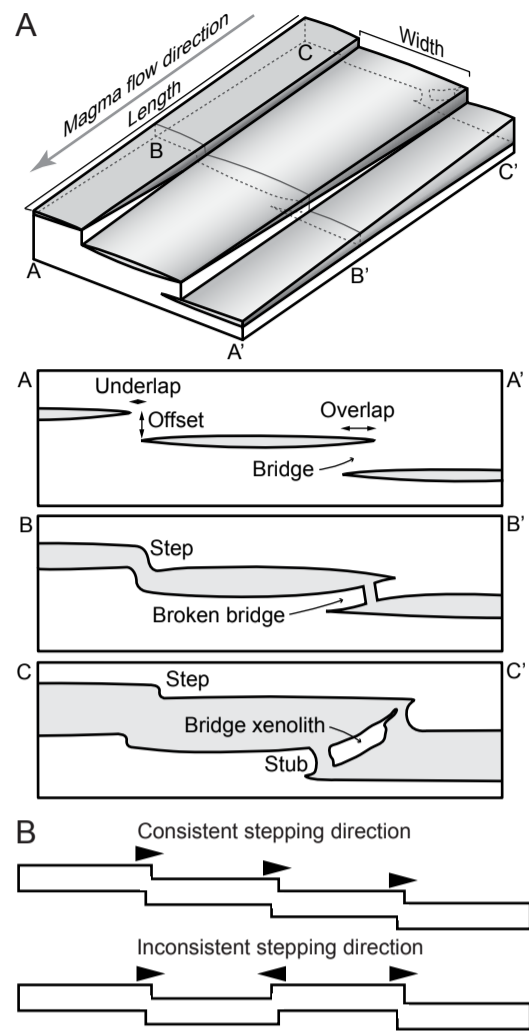


Figure 1: (A) Schematic diagram documenting the description and development of segments connected by steps and bridge structures (redrawn from Magee et al., 2016). (B) Schematic diagram defining consistent and inconsistent stepping directions.

Figure 2

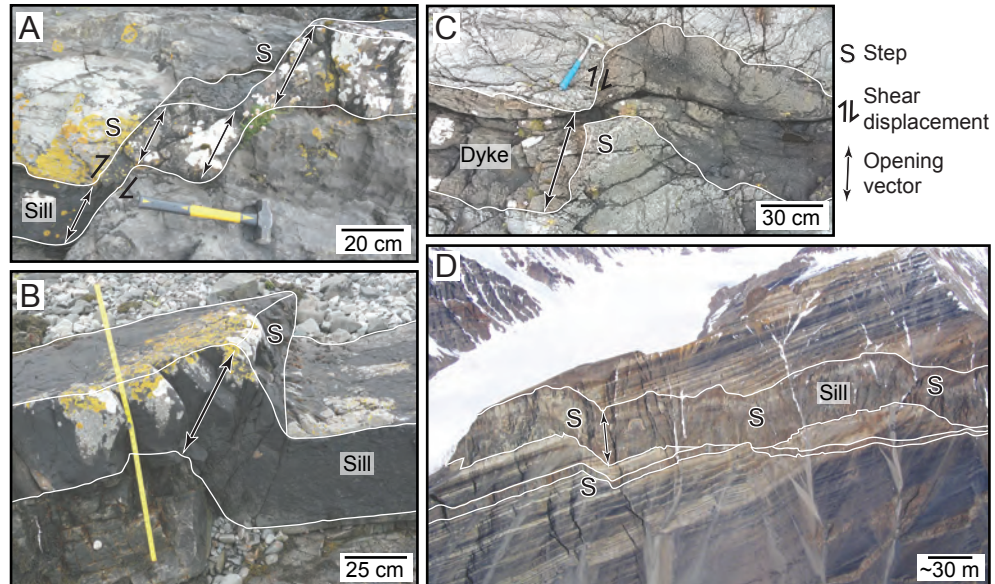


Figure 2: Steps developed in mafic sheets intruding: (A and B) Mesozoic limestone and shale metasedimentary rocks on Ardnamurchan, NW Scotland; (C) Neoproterozoic schists at Mallaig, NW Scotland; and (D) a sedimentary succession on Axel Heiburg island, Canada (photo courtesy of Martin Jackson).

Figure 3

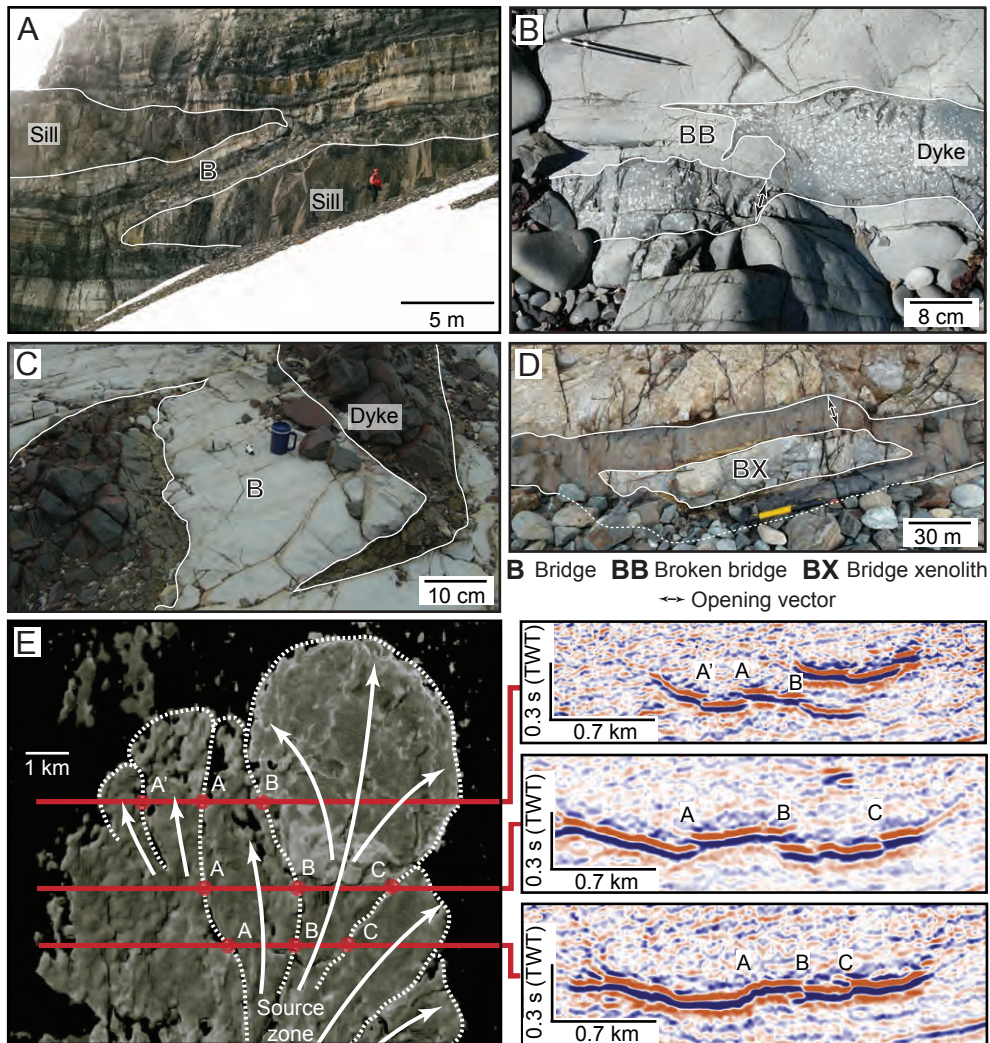


Figure 3: Different bridge structures recorded in mafic intrusions into: (A) Beacon Supergroup sedimentary strata along the Theron Mountains, Antarctica (modified from Hutton, 2009); (B) Beacon Supergroup sedimentary strata along the Allan Hills, Antarctica; (C) a massive dolerite intrusion on Ardnamurchan, NW Scotland; and (D) Mesozoic limestone and shale metasedimentary rocks on Ardnamurchan, NW Scotland. (E) Opacity render of a sill in the Flett Basin, NE Atlantic and corresponding seismic sections detailed intrusive step and broken bridge growth (modified from Schofield et al., 2012b).

Figure 4

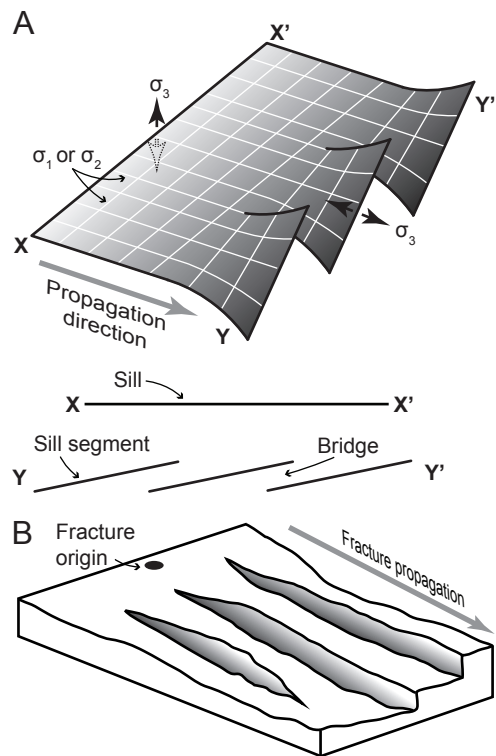


Figure 4: (A) Schematic showing how a change in the principal stress axes can segment a propagating sheet (after Hutton, 2009). (B) Hackle marks developed on a joint plane (redrawn from Kulander et al., 1979).

Figure 5

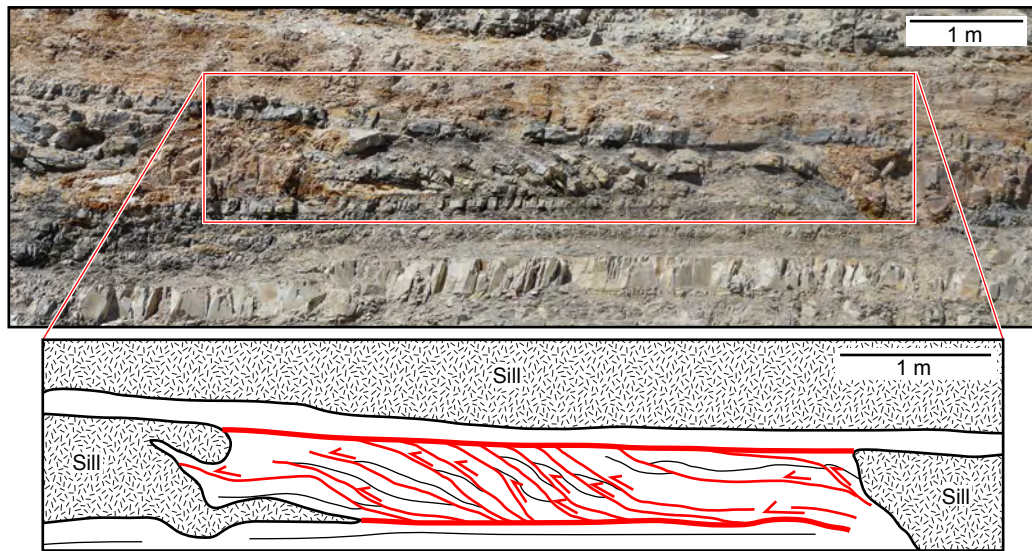


Figure 5: Small-scale imbricate fold and thrust duplex developed due to viscous indentation of finger-like sill intrusions in the Neuquén Basin, Argentina (modified from Spacapan et al., 2017).

Figure 6

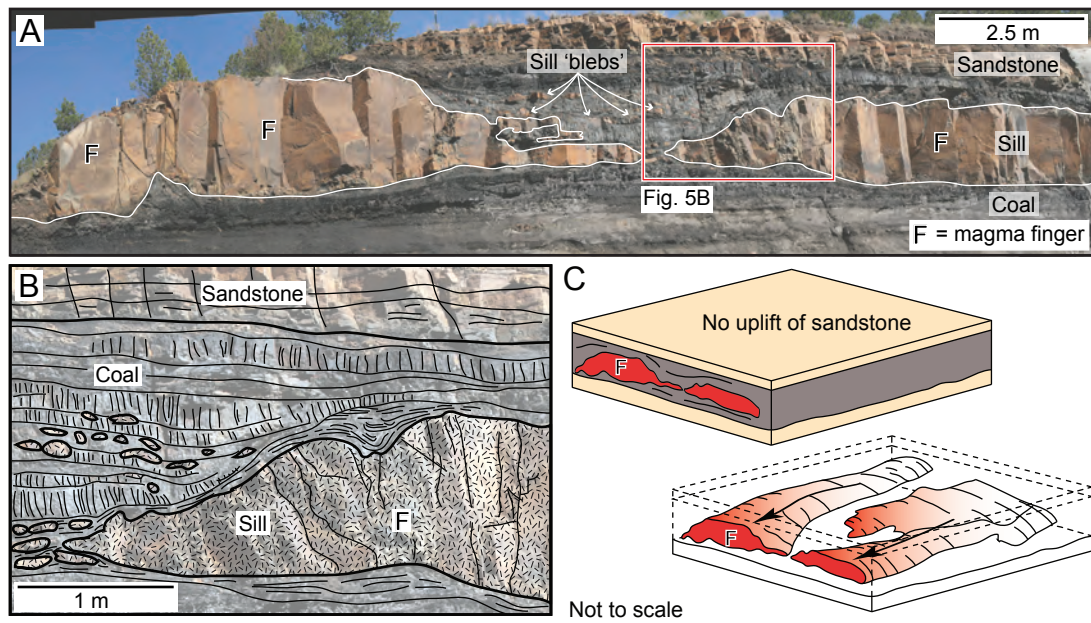


Figure 6: (A and B) Magma fingers developed in response to intrusion-induced heating and plastic deformation of the host rock coals in the Raton Basin, Colorado (modified from Schofield et al., 2012a). (C) Schematic diagrams showing the simplified 3D morphology of the magma fingers in (A and B) (Schofield, 2009).